Quantum-size effects of interacting electrons and holes in semiconductor microcrystals with spherical shape

Yosuke Kayanuma
Department of Physics, Faculty of Science, Tohoku University, Sendai 980, Japan
(Received 2 May 1988)

Quantum-size effects of an electron-hole system confined in microcrystals of semiconductors are studied theoretically with the spherical-dielectric continuum model. An extensive numerical calculation for the eigenvalue problem is carried out by Ritz's variational technique. The motional state of the lowest level is classified into three regimes: the regime of exciton confinement for $R/a_B^* \gtrsim 4$, the regime of individual particle confinement for $R/a_B^* \lesssim 2$, and the intermediate regime for $2 \lesssim R/a_B^* \lesssim 4$, where R is the radius of the quantum well and a_B^* is the exciton Bohr radius. In the region $R/a_B^* \gtrsim 4$, the high-energy shift of the lowest exciton state is described by the rigid-sphere model of the exciton quite well, which takes into account the spatial extension of the relative motion of the electron and the hole. The oscillator strength of the interband optical transition changes dramatically across the region $2 \lesssim R/a_B^* \lesssim 4$. The metamorphosis of the absorption spectrum is shown as a function of R/a_B^* and compared with the experimental data.

I. INTRODUCTION

Quantum-size effects of Wannier excitons in semiconductor microcrystals have been a subject of extensive studies in recent years. A wide variety of materials have been grown as microcrystals in glasses,[1,2] in alkali-halide crystals,[3–9] in liquids,[10–14] and also in vacuum.[15,16] The size quantization effect is most directly detected as the high-energy shift of the interband absorption or luminescence peak in these materials. In addition to the interest in the basic properties of the quasiparticles confined in the three-dimensional quantum well, the potential applicability to the ultrafast nonlinear optical devices seems to have motivated some of the recent investigations.[17–21]

From the theoretical point of view, the ground-state property of an electron and a hole confined in a microcrystal poses a fundamental problem of quantum mechanics: the competition between the attractive two-body force and the one-body force exerted at the well boundary.[22] As noted by Efros and Efros,[23] it can be readily inferred that there are two limiting situations according to the ratio of the characteristic length R indicating the size of the microcrystal to the effective Bohr radius a_B^* of the exciton in the bulk material. In the limit $R/a_B^* \gg 1$, the character of the exciton as *a quasiparticle* is conserved well while the translational degrees of freedom are confined with little energy increment (the regime of the exciton confinement). In the opposite limit $R/a_B^* \ll 1$, the electron and the hole should occupy primarily the individual lowest eigenstate of the quantum well with relatively little spatial correlation (the regime of the individual particle confinement).

According to the wide variation of the dielectric constant and of the effective mass of the electron and the hole, the exciton Bohr radius in real semiconductors covers a fairly wide range; from 7 Å of CuCl to 100 Å of GaAs, for example. One of the central problems is, therefore, to make clear how the motional state of the electron-hole system changes as the ratio R/a_B^* changes continuously and to give the energy of the lowest state as a function of R/a_B^*.

The limit of the strong confinement is relatively easy to handle. Brus[24] derived an expression of the energy of the lowest eigenstate in this limit. On the other hand, the analysis of the weak confinement limit is rather a difficult task because it is not known what to choose as the zeroth-order approximation for the wave function which satisfies the boundary condition. Efros and Efros[23] asserted that the amount of the energy increment in this limit is given just by the value corresponding to that of a single point particle with the mass equal to the total mass of the exciton. Although it is reported that the observed high-energy shift of the exciton absorption[2] and luminescence[8] peak of CuCl microcrystals is explained by this simple picture, further theoretical investigation is required in this limit.

In a previous paper,[25] the present author carried out a simple variational calculation of the ground-state energy of the electron-hole system in a spherical quantum well. The proposed trial wave function, which contains only one parameter, bridges the above-mentioned two limiting cases and naturally covers the whole range of R/a_B^*, where R is the radius of the sphere in this case. It was pointed out that the transition between the two regimes occurs at around $R/a_B^* \simeq 2 \sim 3$ continuously but rather abruptly. However, because of the symmetric form of the assumed trial function under the exchange of the coordinates of the electron and the hole, the energy depends only on the reduced mass of the exciton. It was noted there[25] that, in order to clarify the dependence on the total mass which is important in the weak confinement region, the variational function should be extended to allow

for the asymmetric combination of the coordinates of the two particles.[26]

In the present paper, we study the quantum-size effects of the electron and the hole in a spherical well to the full extent both analytically and numerically. A new type of the variational calculation is developed, which, we believe, gives a very accurate approximation to the exact eigenenergy of the ground state and of the low-lying excited states in a wide range of parameter values. It is proven that the conjecture of Efros and Efros[23] is true in the sense that it gives the lowest-order term of the asymptotic expansion of the high-energy shift in the weak confinement limit. In practice, however, the ground-state energy in the weak confinement region is expressed far better by a formula which takes into account the finiteness of the exciton radius. Not only the ground-state energy but also the level structure of the excited states and the distribution of the oscillator strength for the optical transition are investigated. It will be shown that because of the broken symmetry of the translational degrees of freedom, the optical absorption spectrum of the weakly confined exciton has side bands closely lying above the $1s$ peak and the whole Rydberg series structure gradually changes into the series of well-isolated peaks peculiar to the strong confinement as R/a^* becomes small.

In Sec. II the model is presented. Analytical consideration is given in Sec. III, where we present asymptotic formulas of he ground-state energy in some limiting cases. In Sec. IV the variational method is formulated and the results of the calculation are shown. The discussion is given in Sec. V.

II. MODEL

Let us consider an electron and a hole confined in a microcrystal of spherical shape with the radius R. The microcrystal is approximated by an isotropic continuous medium with the dielectric constant κ. We neglect the effect of the polarization charge induced at the surface[24] for simplicity. It is assumed that the electron and the hole are completely confined in the well by the infinite potential barrier. Our main concern here is to clarify the essential features of the problem by a simplified model, which will serve as a starting point of the analysis in real materials.

The Hamiltonian is given by

$$H=\frac{\mathbf{p}_e^2}{2m_e}+\frac{\mathbf{p}_h^2}{2m_h}-\frac{e^2}{\kappa\,|\,\mathbf{r}_e-\mathbf{r}_h\,|}\ , \tag{1}$$

where $\mathbf{r}_i$, $\mathbf{p}_i$, and m_i are the coordinate, the momentum, and the mass for the electron ($i=e$) and the hole ($i=h$), respectively. The total mass $M\equiv m_e+m_h$ and the reduced mass $\mu\equiv 1/(m_e^{-1}+m_h^{-1})$ will also be used hereafter. The boundary condition is that the wave function Ψ should vanish at $|\,\mathbf{r}_e\,|=R$ and at $|\,\mathbf{r}_h\,|=R$.

From the standpoint of symmetry, our problem is quite analogous to that of the helium atom.[27] The rotational invariance around an arbitrary axis allows us to separate out three angle variables and we are left with only three independent variables relevant to the Schrödinger equation. In carrying out the numerical calculation, the crucial step here is to choose the Hylleraas coordinates,[28] $r_e\equiv|\,\mathbf{r}_e\,|$, $r_h\equiv|\,\mathbf{r}_h\,|$, and $r_{eh}\equiv|\,\mathbf{r}_e-\mathbf{r}_h\,|$ for these variables. The Euler angles determining the plane on which $\mathbf{r}_e$ and $\mathbf{r}_h$ lie can be chosen as the remaining three variables. The eigenstates of the Hamiltonian are classified in accordance with the total angular momentum J, the magnetic quantum number M, and the one additional quantum number k for the vector spherical harmonics.[27] In each subspace of (J,M,k), the Schrödinger equation can be explicitly written down. Throughout the present work, we are solely concerned with the s-like subspace ($J=0$) only to which the interband transition is possible in the direct allowed semiconductors. The Hamiltonian is then greatly simplified as given by the previous paper.[25]

III. ANALYTICAL CONSIDERATIONS

If one adopts the effective Rydberg energy $E_{\mathrm{Ry}}^*\equiv\mu e^4/2\kappa^2\hbar^2$ for the unit of the energy and the effective Bohr radius $a_B^*\equiv\kappa\hbar^2/\mu e^2$ for the unit of the length, the normalized ground-state energy $\varepsilon\equiv E/E_{\mathrm{Ry}}^*$ can be written as a function of two independent dimensionless parameters as

$$\varepsilon=\varepsilon(\sigma,\rho)\ , \tag{2}$$

where $\sigma=m_h/m_e$ is the mass ratio and $\rho\equiv R/a_B^*$. Since $\varepsilon(1/\sigma,\rho)=\varepsilon(\sigma,\rho)$, we assume $\sigma\geq 1$ hereafter.

First of all, the following inequality can be easily proven by using Hellmann-Feynman's theorem,

$$\partial\varepsilon(\sigma,\rho)/\partial\sigma<0\quad\text{for }\sigma\geq 1\ , \tag{3}$$

which means that the ground-state energy is a decreasing function of the total mass for a fixed value of the reduced mass and the well radius.

The asymptotically exact solution for $\varepsilon(\sigma,\rho)$ is obtained in the three limiting cases, $\sigma\to\infty$, $\rho\to\infty$, and $\rho\to 0$.

A. The limit of infinite hole mass

Evidently, the hole resides motionless at the center of the sphere in the limit. Thus the problem reduces to that of the *confined neutral donor* and the Hamiltonian (1) is replaced by that of the hydrogenic donor electron for a single variable r_e.

By following the usual procedure given in textbooks,[29] the Schrödinger equation is transformed into the well-known second-order differential equation which has the regular solution given by the confluent hypergeometric function $M(\nu,2,\xi)$ where $\xi\equiv 2\,|\,\varepsilon\,|^{1/2}r_e/a_B^*$ and $\nu\equiv 1-|\,\varepsilon\,|^{-1/2}$. In the case of a bulk crystal, the energy ε is quantized by the requirement that $M(\nu,2,\xi)$ should become a polynomial (the associated Laguerre polynomial) of ξ so that the wave function vanishes in the limit $r_e\to\infty$. In the present case, ε is quantized as a function of ρ by the requirement that $M(\nu,2,\xi)$ should vanish at $\xi=2\,|\,\varepsilon\,|^{1/2}\rho$. The argument is reversed in the actual calculation. The normalized well radius ρ is calculated as a function of ε by searching the first zero point of $M(\nu,2,\xi)$ which is given by the series expansion,

$$M(\nu,2,\xi)=1+\frac{\nu}{2}\xi+\frac{\nu(\nu+1)}{(2)3}\frac{\xi^2}{2!}+\cdots . \tag{4}$$

Note that the curve $\varepsilon=\varepsilon(\rho)$ passes the points $\varepsilon(2)=-\frac{1}{4}$, $\varepsilon(1.9019\ldots)=-\frac{1}{9},\ldots$. Namely, the $2s,3s,\ldots$ hydrogenic states in the bulk crystal become the $1s$ state in the quantum well when the well surface coincides with the nodal surface of the respective wave functions.

The asymptotic form of the high-energy shift $\Delta\varepsilon(\rho)\equiv 1-|\varepsilon(\rho)|$ in the weak confinement limit $\rho\rightarrow\infty$ is evaluated as follows. Since $\nu\rightarrow 0$ in this limit, $M(\nu,2,\xi)$ is approximated by the first-order expansion in ν. From Eq. (4), we find

$$M(\nu,2,\xi)\simeq 1+g(\xi)\nu , \tag{5}$$

where

$$g(\xi)=\sum_{n=1}^{\infty}\frac{\xi^n}{n!(n+1)!}=\int_0^{\xi}\frac{(e^t-1)}{t}dt-\frac{e^{\xi}-1-\xi}{\xi} . \tag{6}$$

In the limit $\xi\rightarrow\infty$, $g(\xi)$ behaves asymptotically as

$$g(\xi)\simeq\frac{e^{\xi}}{\xi^2} , \tag{7}$$

as can be verified by the partial integration of Eq. (6). From the condition $M(\nu,2,2|\varepsilon|^{1/2}\rho)=0$, we find as the lowest-order correction,

$$\Delta\varepsilon(\rho)\simeq 8\rho^2\exp(-2\rho) , \tag{8}$$

or, by recovering the dimension,

$$\Delta E\simeq 8E^*_{\mathrm{Ry}}(R/a_B^*)^2\exp(-2R/a_B^*) . \tag{9}$$

Physically, the amount of the high-energy shift due to the confinement becomes exponentially small in the limit $\rho\rightarrow\infty$ since the hydrogenic $1s$ wave function decays exponentially.

B. The limit of weak confinement

In the limit $\rho\rightarrow\infty$ with a fixed σ, $\varepsilon(\sigma,\rho)$ should be expanded in a power series of descending order of ρ. One would expect that, to the lowest order,

$$\varepsilon(\sigma,\rho)=-1+\frac{\sigma}{(1+\sigma)^2}\left[\frac{\pi}{\rho}\right]^2 , \tag{10}$$

or

$$E=-E^*_{\mathrm{Ry}}+\frac{\hbar^2}{2M}\left[\frac{\pi}{R}\right]^2 , \tag{11}$$

where the higher-order terms decreases faster than ρ^{-2} or R^{-2}. However, this is by no means a trivial matter since the boundary condition is imposed not on the center-of-mass coordinate but on those of the electron and the hole. The above asymptotic formula is proven as follows.

If one rewrites Eq. (1) in terms of the coordinate and the momentum for the center of mass $(\mathbf{X},\mathbf{P})$ and for the relative motion $(\mathbf{r},\mathbf{p})$, the domain allowed for $\mathbf{r}$ to sweep becomes a complicated function of $\mathbf{X}$ for a fixed value of $|\mathbf{X}|$ $(<R)$. So we replace the original problem by those in which the boundary conditions for $\mathbf{X}$ and $\mathbf{r}$ are decoupled and evaluate the upper and the lower bounds of the ground-state energy E.

First, it is evident that E is bounded from below as

$$-E^*_{\mathrm{Ry}}+\frac{\hbar^2}{2M}\left[\frac{\pi}{R}\right]^2<E , \tag{12}$$

since the left-hand side of the above inequality is just the ground-state energy of (1) with the relaxed boundary condition,

$$|\mathbf{X}|\le R \quad\text{and}\quad |\mathbf{r}|\le\infty . \tag{13}$$

As for the upper bound of E, we consider a new boundary condition that $\mathbf{X}$ and $\mathbf{r}$ are confined as

$$|\mathbf{X}|\le R-d(R) \quad\text{and}\quad |\mathbf{r}|\le d(R) , \tag{14}$$

where $d(R)$ is an increasing function of R to be determined later. Since the condition (14) is more strict than the original one, we obtain

$$E<\frac{\hbar^2}{2M}\frac{\pi^2}{(R-d)^2}+\tilde{E}(d) , \tag{15}$$

where $\tilde{E}(d)$ is nothing but the energy of the hydrogenic donor confined in the sphere with the radius d, which is just given in A. Therefore, in the limit $d/a_B^*\rightarrow\infty$, $\tilde{E}(d)$ tends to $-E^*_{\mathrm{Ry}}$ with the exponentially small correction. Choosing, for example, $d=\sqrt{R}$ as the functional form of $d(R)$ and letting $R/a_B^*\rightarrow\infty$, we obtain the upper bound,

$$E\le -E^*_{\mathrm{Ry}}+\frac{\hbar^2}{2M}\left[\frac{\pi}{R}\right]^2+\cdots , \tag{16}$$

where the correction term goes to zero faster than R^{-2}. Equation (11) readily follows from Eqs. (12) and (16).

The effect of the finiteness of the spatial extension of the exciton, which is neglected in the formula (11), gives the higher-order terms in the asymptotic expansion with respect to R^{-1}. The numerical calculation given in the next section shows that it is not negligible in the region of practical interest and can be included effectively in the renormalization of the well radius.

C. The limit of strong confinement

In the limit $\rho\rightarrow 0$ with a fixed σ, $\varepsilon(\sigma,\rho)$ should be expanded in a power series of ascending order of ρ. The zeroth-order approximation was given by Brus[24] by the wave function which is the product of those for the lowest eigenstate of the individual particle in the spherical well. The present author noted in the previous paper[25] that there remains a finite contribution to the ground-state energy from the spatial correlation effect even in the limit $\rho\rightarrow 0$: the exciton effect persists in the limit of zero dimension because of the divergence of the Coulomb interaction.

The asymptotic wave function is given by

$$\Psi(r_e,r_h,r_{eh})=j_0\left[\frac{\pi r_e}{R}\right]j_0\left[\frac{\pi r_h}{R}\right](1-Cr_{eh}) , \tag{17}$$

where $j_0(x)$ is the zeroth-order spherical Bessel function. The normalization constant is omitted in this section. The constant C is determined analytically to minimize the expectation value of the energy as $C=0.498.../a_B^*$ for which we find[25]

$$\varepsilon(\sigma,\rho)=\left[\frac{\pi}{\rho}\right]^2-\frac{3.572}{\rho}-0.248\ , \tag{18}$$

or

$$E=\frac{\hbar^2}{2\mu}\left[\frac{\pi}{R}\right]^2-1.786\frac{e^2}{\kappa R}-0.248E_{\mathrm{Ry}}^*\ . \tag{19}$$

The formula, including up to the second term has been given by Brus.[24] The third term is the remnant of the exciton effect. A variational calculation using the same type of wave function as Eq. (17) was done also by Schmidt and Weller.[30]

As for the first excited state with s-like symmetry, there are two possible types of the zeroth-order wave function, namely the (s,s) type $\Psi_{s,s}$ and the (p,p) type $\Psi_{p,p}$. The (s,s) type corresponds to the state where the particle with a heavier mass, i.e., the hole, is excited to the second s orbit while the electron resides in the lowest state. The wave function is given by

$$\Psi_{s,s}(r_e,r_h,r_{eh})=j_0\left[\frac{\pi r_e}{R}\right]j_0\left[\frac{2\pi r_h}{R}\right]\ , \tag{20}$$

with the expectation value of the energy,

$$E_{s,s}=\left[\frac{1}{2m_e}+\frac{2}{m_h}\right]\hbar^2\left[\frac{\pi}{R}\right]^2-1.786\frac{e^2}{\kappa R}\ . \tag{21}$$

The (p,p) type is the state in which both particles occupy the lowest p orbit with the total angular momentum equal to zero,

$$\Psi_{p,p}(r_e,r_h,r_{eh})=j_1\left[\frac{\beta r_e}{R}\right]j_1\left[\frac{\beta r_h}{R}\right]\cos\gamma\ , \tag{22}$$

where $j_1(x)$ is the first order spherical Bessel function, $\beta=4.493...$ and $\cos\gamma=(r_e^2+r_h^2-r_{eh}^2)/2r_er_h$. The energy of this state is given by

$$E_{p,p}=\frac{\hbar^2}{2\mu}\left[\frac{\beta}{R}\right]^2-1.884\frac{e^2}{\kappa R}\ . \tag{23}$$

The level ordering depends on the mass ratio σ. Neglecting the small difference in the Coulomb energy, we find the following inequality:

$$E_{s,s}\lesssim E_{p,p}\quad\text{for } 1.9\lesssim\sigma\ . \tag{24}$$

This has an important consequence in the assignment of the absorption peaks in the strong confinement region since $\Psi_{p,p}$ is optical allowed as a final state of the interband transition while $\Psi_{s,s}$ is forbidden because of the orthogonality of $j_0(\pi r_e/R)$ and $j_0(2\pi r_h/R)$.

IV. NUMERICAL RESULTS

A variational calculation of Ritz's type is carried out in order to investigate the whole parameter region. The eigenstate $\Psi(r_e,r_h,r_{eh})$ is expanded in a series of a basis set as

$$\Psi(r_e,r_h,r_{eh})=\sum_{l=0}^{L}\sum_{m=1}^{M}\sum_{n=1}^{N}C_{l,m,n}\phi_m(r_e)\phi_n(r_h)\times\psi_l(r_{eh})\ . \tag{25}$$

The basis function $\phi_m(r_i)$ is chosen as

$$\phi_m(r_i)=\prod_{k=1}^{m}\left[r_i^2-\left[\frac{k}{m}R\right]^2\right],\quad i=e,h \tag{26}$$

which is a $2m$ order polynomial satisfying the boundary condition. As for $\psi_l(r_{eh})$, we assume

$$\psi_l(r_{eh})=r_{eh}^l\exp(-r_{eh}/\alpha)\ . \tag{27}$$

The expansion coefficients $C_{l,m,n}$ and α are the variational parameters to be determined. The optimization process with respect to $C_{l,m,n}$ for a fixed value of α is equivalent to the diagonalization of the Hamiltonian matrix defined by the nonorthogonal basis set $\phi_m(r_e)\phi_n(r_h)\psi_l(r_{eh})$ and can be easily carried out. Then α is varied in order to minimize the lowest eigenenergy. Actually, it is found that the low-lying eigenenergies are insensitive to the variation of α so far as α is varied in the range $a_B^*\lesssim\alpha\lesssim 2a_B^*$. It is expected that the present method gives a very accurate approximation to the true eigenvalue if one include sufficiently large number of basis functions. In the actual calculation, it is found that the lowest eigenvalue converges rather rapidly as the number of basis functions is increased and practically it is sufficient to include $60\sim70$ bases for the parameter values $R/a_B^*\lesssim 20$ and $m_h/m_e\lesssim 10$.

The advantage of our choice of the polynomial basis (26) is that all the matrix elements are calculated by algebraic manipulations without time-consuming multiple numerical integrations. It should be noted that the lowest-order basis function $\phi(r_i)\equiv r_i^2-R^2$ mimics the true one-body eigenfunction $j_0(\pi r_i/R)$ fairly well: The energy expectation value by the former is $(\hbar^2/2m_i)(10.5/R^2)$ which is only 6.4% higher than the exact value $(\hbar^2/2m_i)(\pi/R)^2$.

In Fig. 1 the results of the energy shift in the ground state measured from the value of the bulk exciton are plotted by the solid lines against the well radius with the mass ratio $\sigma\equiv m_h/m_e$ as a parameter. The long-dashed line is the result of the one-parameter theory given in the previous paper.[25] The short-dashed and the dashed-dotted lines represent the asymptotic formulas (19) and (11), respectively. The experimental values obtained from the data of the luminescence of the Z_3 exciton in CuCl microcrystals in NaCl due to Ito *et al.*[8] (○) and the absorption in CdS in glasses due to Ekimov *et al.*[2] (△) are also plotted. In normalizing the data into the dimensionless unit, the following values are used: $E_{\mathrm{Ry}}^*=213$ meV, $a_B^*=7$ Å, and the exciton energy in the bulk crystal 3.218 eV ($T=77$ K) for CuCl (Refs. 31 and 8) and $E_{\mathrm{Ry}}^*=29$

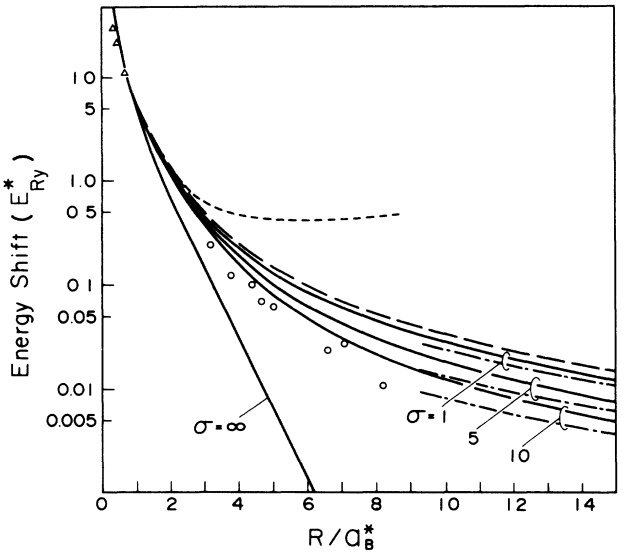

FIG. 1. The calculated high-energy shift of the ground state of the electron-hole system in the spherical quantum well (solid lines) with $\sigma \equiv m_h/m_e$ as a fixed parameter. The short-dashed line and the dashed-dotted lines represent the asymptotic formulas (19) and (11), respectively. The long-dashed line is the result by the one-parameter theory. The observed values of the luminescence peak in the CuCl microcrystal in NaCl (○) and the absorption peak of CdS microcrystals in the silicate glass (△) are also plotted.

meV, $a_B^*=29$ Å, and the exciton energy 2.553 eV for CdS.[32] In Table I the numerical values of the normalized ground-state energy are also tabulated to facilitate the comparison with the experimental data and with other theoretical calculations.

As can be seen from the figure, the one-parameter theory works well for the symmetric case $\sigma=1$. The behavior of the curve $\sigma=\infty$ in the region $R/a_B^* \gtrsim 4$ is well described by the asymptotic formula (9). In the limit $R/a_B^* \to 0$, all lines converge to the universal limit independent of σ which is given by the formula (19) and is shown by the short-dashed line.

In the limit $R/a_B^* \to \infty$, the calculated lines tend to the dash-dotted lines representing the formula (11). It is found, however, that the energy in the weak confinement region can be described far better by the formula

$$E=-E^*_{\mathrm{Ry}}+\frac{\hbar^2}{2M}\frac{\pi^2}{[R-\eta(\sigma)a_B^*]^2}\ , \tag{28}$$

than by (11). In the above equation, $\eta(\sigma)$ is an increasing function of σ of order of unity. In fact, the formula (28) reproduces the numerical value of E surprisingly well for $R/a_B^* \gtrsim 4$ if one chooses $\eta(1)=0.73$, $\eta(3)=1.1$, $\eta(5)=1.4$, etc. In order to see this, the numerical result for $\sigma=3$ is plotted by the solid curve in Fig. 2 in the enlarged scale together with those given by the formula (19) (short-dashed line), by (11) (dashed-dotted line), and by (28) (long-dashed line). Although the present author could not find any analytical proof of the formula (28), nor any simple expression of the functional form of $\eta(\sigma)$, we can conjecture that Eq. (28) is the true asymptotic form of E in the weak confinement limit where the correction term is exponentially small.

Physically, the term $\eta(\sigma)a_B^*$ corresponds to the so-called dead layer:[33] The center of mass of the exciton cannot reach the well surface because it requires a strong deformation in the relative motion of the electron and the hole. The fact that $\eta(\sigma)$ is an increasing function of σ is consistent with this picture since, for a fixed value of a_B^*, the spatial extension of the relative motion around the center of mass increases as the mass ratio becomes larger. It is noticeable that, as far as the ground state is con-

TABLE I. The calculated ground-state energy of the electron-hole system in the spherical quantum well. The energy is measured from the band-gap energy in the bulk crystal and normalized by E^*_{Ry}. The upper limit (L,M,N) of the basis functions included is (3,4,4) for $\sigma=1$ and 3 and (3,3,6) for $\sigma=5$ and 10.

R/a_B^*	$\sigma=1$	$\sigma=3$	$\sigma=5$	$\sigma=10$
0.5	32.03	32.01	31.98	31.90
1	5.974	5.950	5.918	5.841
1.5	1.656	1.631	1.599	1.529
2	0.3045	0.2795	0.2484	0.1841
2.5	−0.2553	−0.2797	−0.3089	−0.3646
3	−0.5290	−0.5522	−0.5786	−0.6261
3.5	−0.6789	−0.7004	−0.7239	−0.7639
4	−0.7684	−0.7880	−0.8085	−0.8421
5	−0.8640	−0.8797	−0.8952	−0.9189
6	−0.9108	−0.9231	−0.9349	−0.9521
7	−0.9371	−0.9469	−0.9559	−0.9687
8	−0.9533	−0.9612	−0.9683	−0.9780
9	−0.9639	−0.9704	−0.9760	−0.9837
10	−0.9713	−0.9767	−0.9813	−0.9875
15	−0.9879	−0.9926	−0.9926	−0.9953
20	−0.9933	−0.9948	−0.9960	−0.9975

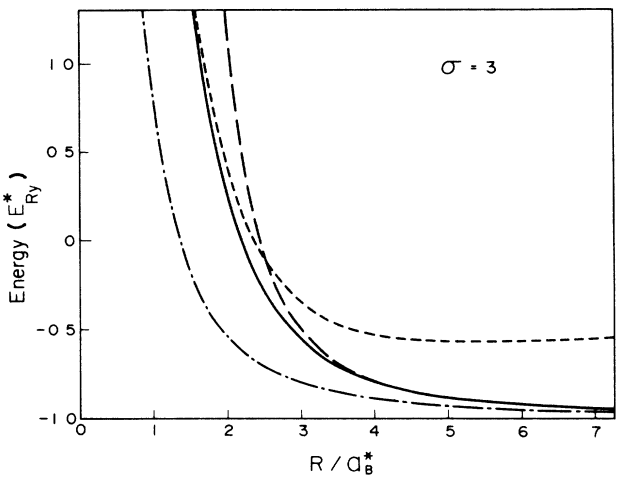

FIG. 2. The comparison of the calculated ground-state energy (solid line) with the asymptotic formula (19), short-dashed line; formula (11), dashed-dotted line; and formula (28), long-dashed line with $\eta(3)=1.1$.

cerned, the exciton behaves like a rigid sphere even in such a small size of quantum well as $R/a_B^* \simeq 4$.

From Figs. 1 and 2 we conclude that the transition from the exciton confinement regime to the individual particle confinement regime occurs continuously but rather distinctly in the region $2 \lesssim R/a_B^* \lesssim 4$. The same conclusion has been drawn in the previous paper[25] by observing the change in the relative motion.

The metamorphosis of the motional state of the confined electron-hole system is also exhibited in the energy scheme of the excited states. In Fig. 3 the energy of the lowest 12 s-like eigenstates is plotted against the well radius. One can clearly recognize that there are two types of excitations in the weak confinement region: One is the excitation of the center-of-mass motion and the other is the excitation of the relative motion to the hydrogenic $2s, 3s, \ldots$ states. As R/a_B^* becomes smaller, these two types of the excited levels undergo quasicrossings and are hybridized with each other. The first excited state of the center-of-mass motion changes into the (s,s)-type state given in Eq. (20) in the strong confinement limit.

In the bulk crystal of semiconductors with the direct allowed gap, the optical absorption occurs only to the s-like excitonic levels (including the ionization continuum) with the zero translational wave vector because of the momentum conservation. In the spherical quantum well with a finite size, all the s-like states become optical allowed in principle because of the breakdown of the translational invariance. In order to see how the absorption spectrum changes as a function of R/a_B^*, we have calculated the oscillator strength f_j of jth level per unit volume in accordance with the formula[34]

$$\frac{f_j}{f_{ex}} = \frac{\pi a_B^{*3}}{V} \left| \int \Psi_j(r,r,0) d^3r \right|^2 , \tag{29}$$

where f_{ex} is the oscillator strength of the $1s$ exciton in the bulk crystal per unit volume, V is the volume of the microcrystal, and Ψ_j is the wave function of the jth level. The term proportional to the photon energy is omitted here.

In Fig. 4 an example of the calculated absorption spectrum is shown for $\sigma=5$. The result for $R/a_B^*=10$ shows the confinement induced redistribution of the oscillator strength of the $1s$ exciton to the closely lying excited states of the center-of-mass motion. In the limit $R/a_B^* \to \infty$, the oscillator strength of the infinite number of excited states of the center-of-mass motion accumulate to those of the hydrogenic $1s, 2s, \ldots$ thus recovering the Rydberg series of the bulk exciton absorption spectrum which obeys the well-known n^{-3} rule of the intensity ratio.[35]

In the strong confinement region, f_1 increases and diverges as

$$f_1 \simeq \frac{3}{4} \left(\frac{a_B^*}{R} \right)^3 f_{ex} , \tag{30}$$

because of the strong overlapping of the wave functions of the confined electron and hole. Note the change in the scale of the ordinate and the abscissa in the lowermost figure. In this case, the first excited state at around $E \simeq 11 E^*_{Ry}$ has only a negligible intensity because this state tends to the (s,s)-type forbidden state as noted earlier.

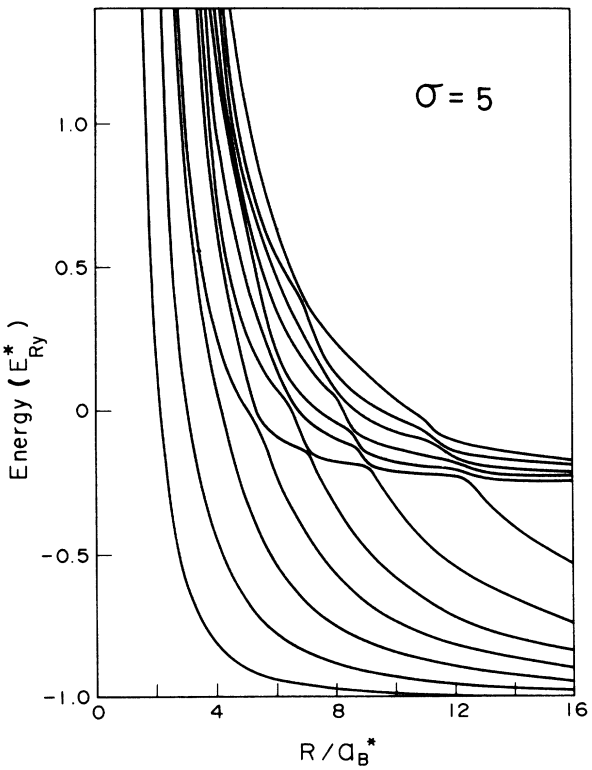

FIG. 3. The energy levels of the s-like state for $\sigma=5$. Only the lowest 12 levels are plotted.

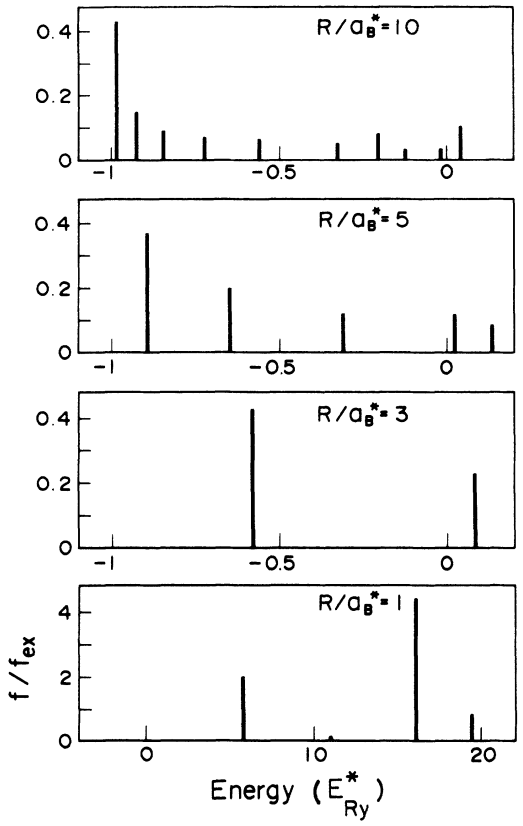

FIG. 4. The interband absorption spectrum in the spherical microcrystal with $\sigma=5$ as a function of the well radius. The ordinate represents the oscillator strength per unit volume normalized by that of the free exciton.

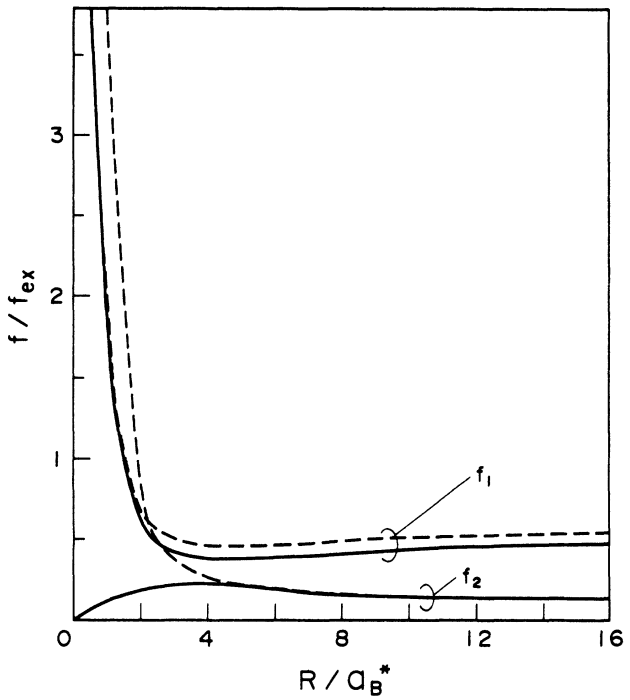

FIG. 5. The normalized oscillator strength of the ground (f_1) and the first excited (f_2) states per unit volume. The solid lines and the dashed lines are the results for $\sigma=5$ and $\sigma=1$, respectively.

In Fig. 5 the dependence of f_1 and f_2 on R/a_B^* is shown for $\sigma=5$ (solid lines) and for $\sigma=1$ (dashed lines). Although the behavior of f_1 is very similar for both cases, that of f_2 becomes quite different in the region $R/a_B^* \lesssim 4$. Unlike the case for $\sigma=5$, f_2 for $\sigma=1$ diverges as

$$f_2 \simeq \frac{9}{4}\left[\frac{a_B^*}{R}\right]^3 f_{\rm ex} , \tag{31}$$

in the limit $R/a_B^* \to 0$ since this state tends to the (p,p)-type state given by Eq. (22).

In Fig. 6 the oscillator strength of the ground state *for a microcrystal* Vf_1 normalized by $a_B^{*3} f_{\rm ex}$ is given against R/a_B^* in the logarithmic scale. In the region $R/a_B^* \gtrsim 4$, the oscillator strength increases proportionally to R^3 as indicated by the straight line. This is nothing but the effect of the giant oscillator strength first proposed by Rashba and Gurgenishvili[36] for the bound exciton. For $R/a_B^* \lesssim 2$, the calculated value deviates significantly from the dashed line and tends to the asymptotic value π indicated by the small arrow in the limit $R/a_B^* \to 0$. Here we see the transition from the exciton confinement regime to the individual particle confinement regime again.

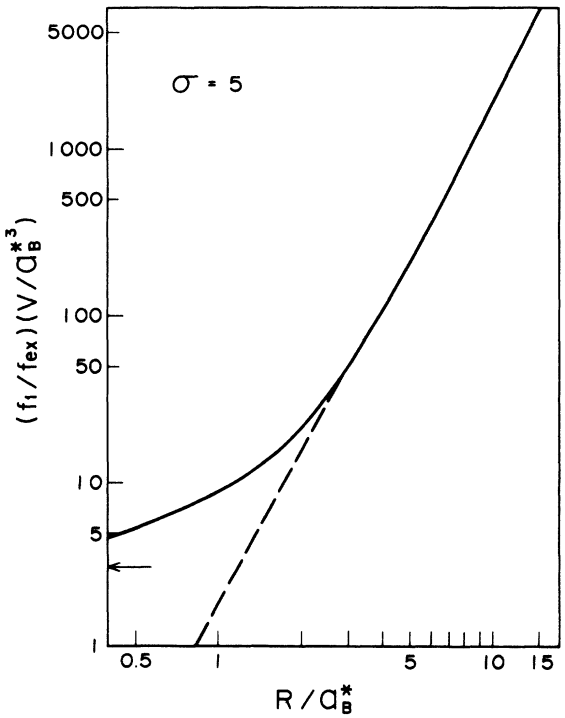

FIG. 6. The normalized oscillator strength of the ground state for a microcrystal in the case $\sigma=5$. The dashed line indicates the asymptotic value for $R/a^* \gg 1$ and is proportional to R^3.

V. DISCUSSION

As shown in Fig. 1 the microcrystals of CuCl and of CdS present typical examples of the weak confinement and of the strong confinement, respectively. The theoretical curves reproduce the overall size dependence of the high-energy shift fairly well. Quantitatively, the calculated values are somewhat larger than those observed.

In the case of CuCl, Ekimov *et al.*[2] and Itoh *et al.*[8,9] noted that the experimental values are fitted by the point particle formula (11). If one fixes $a_B^*=7$ Å, one must take $\sigma \simeq 15$ in order to reproduce the observed value within the present model, which is too large as compared with the value $\sigma=3\sim4$ estimated from the values $\mu=0.39m_0$ (Ref. 31) and $M=2.0m_0$ (Ref. 37) or $M=2.3m_0$,[38] where m_0 is the electron mass in vacuum.

One of the effects which may explain the reduction of the observed high-energy shift is the incomplete confinement due to the finiteness of the potential barrier at the well surface. According to the preliminary result of a variational calculation,[39] the high-energy shift of the exciton in CuCl:NaCl is reduced to about 80% of the values given by the infinite barrier model in the range $3 \lesssim R/a_B^* \lesssim 10$ if one takes into account the finite potential gap estimated for this material. Details will be published elsewhere.

We would like to point out here an alternative and probably more plausible explanation of the discrepancy. As can be seen from Fig. 1, the experimental data for CuCl are well fitted by the theoretical curve if one tentatively normalizes the data using $a_B^*=5.5$ Å instead of $a_B^*=7$ Å. In view of the fact that the lattice constant of CuCl in the γ phase is 5.4 Å, the continuum model will not be fully justified for such a small size of exciton. However, we suspect that the above-mentioned fact is an indication that the exciton in CuCl has a more compact envelope function than has been supposed so far.

As for the case of CdS, the present model predicts the lowest absorption peak at 2.92, 3.52, and 4.12 eV for the size of microcrystals $R=23$, 15, and 12 Å, respectively. The experimental data by Ekimov *et al.*[2] for the samples with corresponding averaged sizes of microcrystals show the lowest peak at around 2.9, 3.2, and 3.5 eV, respectively. The main origin of the deviation from the theoretical value which becomes salient in the smaller size of microcrystals may be the effect of the incomplete confinement. Note that the ground-state energy of the confined electron and hole should actually tend to that of the exciton of the matrix material in the limit $R/a_B^* \to 0$ instead of increasing infinitely. The second peak observed in the sample with $R=15$ Å can be assigned as the (p,p)-type second excited state (see Fig. 4).

It will be worthwhile to detect experimentally the transition between the exciton confinement regime and the individual particle confinement regime by covering a suitable range of R/a_B^* with a single sort of material. As has been shown in the present paper, this transition is more clearly exhibited in the change of wave function than in the shift of the energy. According to Fig. 6, the radiative lifetime of the exciton in the weak confinement region should decrease rapidly as the size of the microcrystal increases so far as the coherence of the wave function is maintained throughout the quantum well. On the other hand, the lifetime depends only weakly on the size of the microcrystal in the strong confinement region through the variation of the transition energy as pointed out by Brus.[24] Furthermore, Fig. 5 tells us that the absorption coefficient of the materials containing microcrystals *with a fixed value of doping* is nearly constant in the region of weak confinement but increase sharply as we enter into the strong confinement region. These features can be used as experimental landmarks of the transition between the two regimes.

In the present model, the shape of the microcrystal is assumed to be a perfect sphere. The deviation from the spherical shape which must exist in real materials will lead to the relaxation of the selection rule as well as the modification of the energy scheme. The shape dependence of the quantum-size effect should be studied theoretically.

As shown in Fig. 3 the electronic structure of the valence band and the conduction band is strongly modified in the small size of microcrystals. In some cases, this will cause an appreciable change in the dielectric constant. In such cases, κ itself should be calculated self-consistently. This is also left for future work.

ACKNOWLEDGMENTS

I would like to thank Professor T. Itoh for valuable discussions and for sharing the experimental data before publication. I am also grateful to Professor A. Nakamura of Nagoya University for useful information.

[1] A. I. Ekimov and A. A. Onushchenko, Fiz. Tekh. Poluprovodn. **16**, 1215 (1982) [Sov. Phys.—Semicond. **16**, 775 (1982)].
[2] A. I. Ekimov, Al. L. Efros, and A. A. Onushchenko, Solid State Commun. **56**, 921 (1985).
[3] S. Nagasaka, M. Ikezawa, and M. Ueta, J. Phys. Soc. Jpn. **20**, 1540 (1965).
[4] H. Kishishita, Phys. Status Solidi B **55**, 399 (1973).
[5] T. Tsuboi, J. Chem. Phys. **72**, 5343 (1980).
[6] T. Itoh and K. Kirihara, J. Lumin. **31/32**, 120 (1984).
[7] C. Zaldo and F. Jaque, J. Phys. Chem. Solids **46**, 689 (1984).
[8] T. Itoh, Y. Iwabuchi, and M. Kataoka, Phys. Status Solidi B **145**, 567 (1988).
[9] T. Itoh, Y. Iwabuchi, and T. Kirihara, Phys. Status Solidi B **146**, 531 (1988).
[10] G. C. Papavassilious, J. Solid State Chem. **40**, 330 (1981).
[11] R. Rossetti, R. Hull, J. M. Gibson, and L. E. Brus, J. Chem. Phys. **82**, 552 (1985).
[12] N. Chestnoy, R. Hull, and L. E. Brus, J. Chem. Phys. **85**, 2237 (1986).
[13] H. Weller, H. M. Schmidt, U. Koch, A. Fojtic, S. Barel, A.

Henglein, W. Kunath, K. Weiss, and E. Dieman, Chem. Phys. Lett. **124**, 557 (1986).
[14]C. J. Sandroff, D. M. Hwang, and W. M. Chung, Phys. Rev. B **33**, 5953 (1986).
[15]S. Hayashi and R. Ruppin, J. Phys. C **18**, 2583 (1985).
[16]S. Hayashi and K. Yamamoto, J. Phys. Soc. Jpn. **56**, 2229 (1987).
[17]G. Bret and F. Gires, Appl. Phys. Lett. **4**, 175 (1964).
[18]R. K. Jain and R. C. Lind, J. Opt. Soc. Am. **73**, 647 (1982).
[19]S. S. Yao, C. Karaguleff, A. Gabel, R. Fortenberry, C. T. Seaton, and G. I. Stegeman, Appl. Phys. Lett. **46**, 801 (1985).
[20]J. Warnock and D. D. Awschalom, Phys. Rev. B **32**, 5529 (1985).
[21]G. R. Olbright and N. Peyghambarian, Appl. Phys. Lett. **48**, 1184 (1986).
[22]D. C. Mattis and G. Beni, Phys. Rev. B **18**, 3816 (1978).
[23]Al. L. Efros and A. L. Efros, Fiz. Tekh. Poluprovodn. **16**, 1209 (1982) [Sov. Phys.—Semicond. **16**, 772 (1982)].
[24]L. E. Brus, J. Chem. Phys. **80**, 4403 (1984); **90**, 2555 (1986).
[25]Y. Kayanuma, Solid State Commun. **59**, 405 (1986).
[26]A slightly improved variational calculation has recently been done by S. V. Nair, S. Sinha, and K. C. Rustagi, Phys. Rev. B **35**, 4098 (1987).
[27]With respect to the helium atom see, for example, A. K. Bhatia and A. Temkin, Rev. Mod. Phys. **36**, 1050 (1964).
[28]E. A. Hylleraas, Z. Phys. **54**, 347 (1929).
[29]L. I. Schiff, *Quantum Mechanics*, 2nd ed. (McGraw-Hill, New York, 1968), p. 80.
[30]H. M. Schmidt and H. Weller, Chem. Phys. Lett. **129**, 615 (1986).
[31]S. Nikitine, Prog. Semicond. **6**, 269 (1962).
[32]B. Segall and D. T. F. Marple, in *Physics and Chemistry of II-VI Compounds*, edited by M. Aven and J. S. Prener (North-Holland, Amsterdam, 1967), Chap. 7, p. 317.
[33]J. J. Hopfield and D. G. Thomas, Phys. Rev. **132**, 563 (1963).
[34]C. H. Henry and K. Nassau, Phys. Rev. B **1**, 1628 (1969).
[35]R. J. Elliott, Phys. Rev. **108**, 1384 (1957).
[36]E. I. Rashba and G. E. Gurgenishvili, Fiz. Tverd. Tela (Leningrad) **4**, 1029 (1962) [Sov. Phys.—Solid State **4**, 759 (1962)].
[37]Y. Masumoto, Y. Unuma, Y. Tanaka, and S. Shionoya, J. Phys. Soc. Jpn. **47**, 1844 (1979).
[38]T. Mita, K. Sotome, and M. Ueta, Solid State Commun. **33**, 1135 (1980).
[39]Y. Kayanuma and H. Momiji (unpublished).